

Unpublished GENOPT/BIGBOSOR4 “balloon” report, February 2011

USE OF GENOPT AND BIGBOSOR4 TO OBTAIN OPTIMUM DESIGNS OF MULTI-WALLED INFLATABLE SPHERICAL AND CYLINDRICAL VACUUM CHAMBERS

David Bushnell, retired, 775 Northampton Drive, Palo Alto, CA 94303

(This is an abridged version. See the full-length paper for more: genopt.papers/2011.balloon.pdf)

GENOPT/BIGBOSOR4 is applied to the problem of perfect elastic spherical or cylindrical “shells” the complex inflatable wall of which is a webbed sandwich. The spherical or cylindrical “shell” is stabilized by uniform pressure applied between its inner and outer walls and subjected to uniform pressure applied to its outermost wall. This paper is analogous to [1]. The distance between the inner and outer walls of the optimized spherical balloons is smaller than that for the optimized cylindrical balloons. The pre-buckling behavior of the spherical balloons is “crankier” (more nonlinear) than that of the cylindrical balloons with the result that certain special strategies have to be introduced in order to permit the generation of optimum designs via the GENOPT processor called SUPEROPT. General buckling modes of the type observed in optimized cylindrical balloons have so far not been observed in any spherical balloons, optimized or not. Local buckling modes include both axisymmetric modes and non-axisymmetric modes with many circumferential waves. Since [1] was written new versions of the “balloon” software, behavior.balloon and bosdec.balloon, have been created by means of which both cylindrical and spherical balloons and balloons with either radial webs or truss-like (slanted) webs can all be optimized and analyzed with use of the same “balloon” software. Since [1] was produced a new behavioral constraint has been added that involves a load factor corresponding to the initial loss of tension in any of the segments of the balloon wall. This new behavioral constraint is related to initial wrinkling of the balloon, which is a type of buckling that pertains to both cylindrical and spherical balloons. Optimum designs are found for balloons made of polyethylene terephthalate, which has a maximum allowable stress of 10000 psi and weight density, 0.1 lb/in³, and for balloons made of a much stronger and lighter fictitious carbon fiber cloth, which has much higher maximum allowable tensile and compressive stresses, 75600 psi and 59600 psi, respectively, and lower weight density, 0.057 lb/in³. The optimized weights of the balloons made of the much stronger and lighter fictitious carbon fiber cloth are 15 to 20 times lighter than those made of polyethylene terephthalate. A section is included showing optimized designs of cylindrical balloons made of the fictitious carbon fiber cloth, which is not included as a material option in [1]. Some peculiarities of the pre-buckling deformations and general buckling modes of optimized spherical and cylindrical balloons made of fictitious carbon fiber cloth are displayed. These optimized balloons, which have much thinner walls than the optimized balloons made of polyethylene terephthalate, exhibit significant spurious local “zig-zag” components of pre-buckling and bifurcation buckling modal displacements. Convergence studies with respect to the number of nodal points used for each segment of the balloons indicate that this spurious local “zig-zag” characteristic does not have a major influence on the prediction of the overall behavior of the balloons. Therefore, it appears that the optimized designs are valid despite the spurious local “zig-zag” characteristic, which disappears with increasing numbers of nodal points used in each segment of a balloon wall.

SECTION 1 INTRODUCTION, PURPOSE, AND SUMMARY

1.1 Introduction and purpose

The effort that resulted in [1] and in this paper was motivated by Michael Mayo, Lockheed Martin Advanced Technology Center, Palo Alto, California, who found Ref.[2]. In [2] the stability of a multi-walled cylindrical vacuum chamber of one of the types treated in [1] is investigated: the cylindrical balloon with radial webs (Fig. 1 of [1]). The aim of the analysis in [2] is to determine the pressure between the inner and outer walls such that the cylindrical vacuum chamber subjected to a given external pressure will remain stable.

The purpose of the work reported in the present paper is to expand the generic “balloon” capability described in [1] to optimize (find the minimum weight of) not only cylindrical vacuum chambers but also of spherical vacuum chambers with walls of the types depicted in Fig. 1 and in Fig. 7(a) of [2]. Figures 1 and 2 of [1] show the geometries of the cross sections of 90 degrees of the circumference of a cylindrical vacuum chamber that are analogous to those shown in Fig. 1 of [2] and in Fig. 7(a) of [2], respectively. Figures 1 and 2 of the present paper show the geometries of the cross sections of 90 degrees of the meridian of a spherical vacuum chamber that are analogous to Figs. 1 and 2 of [1].

It is emphasized that the spherical vacuum chamber, frequently called “spherical balloon” in this paper, has no meridionally oriented webs or gores, only circumferentially oriented webs as displayed in Figs. 1 and 2. The outer wall of the spherical balloon has axisymmetric local bulges reminiscent of the Michelin Tire Man, not the meridionally oriented bulging gores typical of those in recreational balloons, the kind that lift tourists in baskets suspended beneath them. The BIGBOSOR4 model [4,5,6], on which this study is based, cannot handle shells or balloons with meridionally oriented bulging gores or meridionally oriented webs because structures of those types are not axisymmetric, and BIGBOSOR4 is a shell-of-revolution analyzer. The spherical vacuum chamber (balloon) reminiscent of the Michelin Tire Man is not isotropic. Hence, when the pressure, PMIDDLE, is applied between the inner and outer walls, the initially spherical balloon elongates much more in the axial (vertical) direction than in the radial direction, becoming very slightly egg-shaped, as is displayed in Fig. 6 of the complete paper, for example.

The reader should first read [1] in order more fully to understand the technology on which the present paper is based. Some of the details in [1] will not be repeated here. For example, the section in [1] about prismatic shells is not relevant to spherical vacuum chambers, which are modeled as “ordinary” shells of revolution.

To solve the problem for a given balloon wall cross section and to provide a means to optimize that wall cross section, the GENOPT system [3] is combined with the most recent version of the BOSOR4 code [4,5], a shell-of-revolution analyzer called “BIGBOSOR4” [6]. BIGBOSOR4 handles many more shell segments (up to 295 shell segments) than does the much older BOSOR4. In this paper the system created to optimize shells of revolution is called “GENOPT/BIGBOSOR4” [6 – 9]. A brief overview of the GENOPT program [3] is given in [1] and repeated here (in the complete paper) because the reader needs that information in order to understand how GENOPT works. Extensive details about how to use GENOPT in connection with BIGBOSOR4 are presented in [7], [9], and [13].

The GENOPT computer program [3] performs optimization with the use of a gradient-based optimizer called “ADS”, created many years ago by Vanderplaats and his colleagues [10,11]. In [3] and [6 – 9] ADS is “hard wired” in a “modified-method-of-steepest-descent” (1-5-7) mode. In GENOPT a matrix of behavior constraint gradients is computed from finite differences of the behavioral constraints for the perturbed design minus the behavioral constraints for the current design in which the decision variables are perturbed one at a time by a certain percentage, usually five per cent. By “behavior” is meant buckling, stress, displacement, vibration frequency, clearance, and any other phenomena that may affect the evolution of a design during optimization cycles. In this paper the behavioral constraints are bifurcation buckling, initial loss of tension in the balloon wall, and stress.

The objective of the optimization is to minimize the weight of a spherical or a cylindrical vacuum chamber subjected to a set of specified requirements: behavioral constraints such as buckling, loss of tension, and stress.

The models used here for the optimization of the sandwich wall are BIGBOSOR4 models [4,5,6]. Therefore, the discretization is one-dimensional (strip method), which causes solution times on the computer to be much less than for the usual two-dimensionally discretized finite-element models generated in general-purpose finite-element computer programs for the analysis of structures. This property of one-dimensional discretization leads to efficient optimization. Even so, computer run times for “global” optimization via the GENOPT processor

called “SUPEROPT” [12] are long, especially for configurations with many modules, such as that displayed in Fig. 24, for example. The one-dimensional discretization is in the plane of the cross section of the wall of the balloon, as displayed in Figs. 3 and 4, for examples. The variation in the direction normal to the plane of the paper (in the circumferential direction in the case of a spherical balloon and along the axis of the prismatic shell in the case of a cylindrical balloon) is trigonometric with n or N circumferential waves [4,5].

Since [1] was written there have been many changes in the definition of the problem and in the software, behavior.balloon (Table 5) and bosdec.balloon (Table 7), on which the analysis and optimization are based. Now the same generic “**balloon**” software treats both cylindrical and spherical balloons and wall configurations with either radial webs (Fig. 1) or truss-like (slanted) webs (Fig. 2). A new behavioral constraint, the load factor at which the pre-buckling tension in one or more of the segments of the model first goes to zero, has been introduced. This new “loss of tension” (wrinkling) constraint is present both for the cylindrical and for the spherical balloons. Hence, the results presented in [1] are now out of date. Since the “initial loss of pre-buckling tension” constraint has a value that is close to the bifurcation buckling constraint, the results presented in [1] are still approximately correct. The “initial loss of pre-buckling tension” constraint is usually somewhat more critical than the bifurcation buckling constraint. Hence, the latest “**balloon**” software would probably generate slightly heavier optimum designs of the cylindrical vacuum chambers than those reported in [1].

1.2 Summary

In Section 2 of the complete paper a brief summary of GENOPT is given. Section 3 of the complete paper describes how GENOPT is used to create a program system for the optimization of structures that belong to the generic class called “**balloon**” in this paper. Material properties, geometry, and decision variable candidates are introduced in Section 4 of the complete paper. Section 5 of the complete paper identifies the tasks to be performed by a person called here “**the end user**”. Details of results for a particular optimized spherical balloon are explained in Section 6 of the complete paper. Section 7 of the complete paper enumerates and discusses how the models created here differ from those described in [1]. Results for optimized spherical balloons made of polyethylene terephthalate are presented in Section 8 of the complete paper. Section 9 of the complete paper and its several sub-sections give results for optimized spherical balloons made of a fictitious carbon fiber cloth, discuss real and spurious bifurcation buckling modes and real and spurious axisymmetric pre-buckling behavior, demonstrate the presence of meridional stress concentrations at junctions between segments of the complex balloon wall, discuss the convergence of predictions with respect to the number of nodal points used in one or more of these segments, identify the difficulty of finding a “global” optimum design caused by the sometimes frequent failure of Newton convergence in the attempt to find solutions of the nonlinear pre-buckling equilibrium equations during optimization cycles, and describe the sensitivity of optimized designs to changes in certain of the decision variables. Section 10 of the complete paper, analogous in some ways to Section 9 of the complete paper, presents results for optimized cylindrical balloons made of fictitious carbon fiber cloth, a material that is not introduced in [1].

Selected Results from the complete paper:

Figures 10a, 23, 24, 28, 56, and 65 are taken from the complete paper. Explanations appear in the figure captions.

Conclusions (as listed in the complete paper)

The following conclusions may be drawn:

- 1.** No general buckling mode was ever discovered for the spherical balloons analogous to the general buckling modes found for the cylindrical balloons, such as the modes displayed in Figs. 11 and 20 of [1] and in Figs. 57 and 62 of this paper.
- 2.** In cylindrical balloons the lightest optimized designs are those with truss-like (slanted) webs (Fig. 56). In contrast, with spherical balloons the lightest optimized designs are those with radial webs (Fig. 28).
- 3.** In spite of the fact that the segments of the balloon wall behave like membranes that have no bending stiffness rather than like shells that have a finite bending stiffness, BIGBOSOR4, a shell-of-revolution code, which is designed to handle segmented shell structures with finite bending stiffness, seems to be capable of solving both the nonlinear pre-buckling phase and the linear bifurcation buckling phase of the analysis with adequate accuracy for the purpose of preliminary design. However, read the next item.
- 4.** For the balloons made of carbon fiber cloth, both the axisymmetric pre-buckling deformation (Figs. 33a, 34, 35, 55) and the bifurcation buckling modal deformation (Figs. 30, 32, 60) of optimized balloons may exhibit significant components of spurious local “zig-zag” deformation. The amplitude of this spurious component decreases with increasing number of nodal points in each “shell” segment (Fig. 59). Convergence studies indicate that the presence of these spurious local “zig-zag” components does not seriously affect the overall pre-buckling predictions (Figs. 36, 39, Tables 16, 17, 21, 22) and bifurcation buckling predictions (Tables 16, 17, 21, 22) for the spherical and cylindrical balloons. Therefore, it appears that the optimum designs obtained here are valid even though the number of nodal points used in each “shell” segment in the optimization model (31 nodal points, as specified in SUBROUTINE BOSDEC – Table 7) leads to the generation of significant local “zig-zag” deformations in the optimized balloons made of carbon fiber cloth.
- 5.** The balloons made of the fictitious carbon fiber cloth are a factor of 15 – 20 times lighter than those fabricated with polyethylene terephthalate. For optimized spherical balloons compare Fig. 28 with Fig. 23. For optimized cylindrical balloons compare Fig. 56 with Fig. 25 of [1].
- 6.** A strategy is established by means of which failure of convergence of the nonlinear pre-buckling analysis is minimized. This strategy is described in [1].
- 7.** A strategy is established by means of which failure of convergence of the nonlinear pre-buckling analysis does not cause early termination of an execution of SUPEROPT. This strategy is described in Item 7d of Table 8 and in Section 7. For a spherical balloon with truss-like webs this strategy may be invoked many times during an execution of SUPEROPT (Figs. 52a and 52b), which makes it difficult to find a “global” optimum design.
- 8.** Stress components in the various segments of a module are computed from membrane theory, that is, the stress component is equal to the appropriate stress resultant divided by the thickness of the segment (Item No. 11 in Table 9). This is an unconservative strategy because there exist large meridional stress concentrations in the immediate neighborhoods of segment junctions (Fig. 44). An actual balloon fabricated in a configuration that corresponds to an optimized design developed here by GENOPT/BIGBOSOR4 should therefore have reinforced seams at the junctions between segments. The analysis of balloons with reinforced seams is beyond the scope of this paper.
- 9.** The new “initial loss of tension” behavioral constraint called “TENLOS”, which is a predictor of initial wrinkling of the skin in one or more of the segments of the model of the balloon, is close in value to the

bifurcation buckling constraint, BUCKB4, as it should be, since wrinkling is a type of buckling. See Item 1 in Section 9.5 for a spherical balloon and Item 1 in Section 10.2 for a cylindrical balloon.

10. The capability to analyze and design multi-walled spherical and cylindrical vacuum chambers (balloons) is established within the GENOPT/BIGBOSOR4 framework. Enough information is provided in this paper and in [1], [3], [6 – 9], and [13] so that researchers can use GENOPT/BIGBOSOR4 to analyze and design other shell structures of a similar nature.

11. The “balloon” software, behavior.balloon and bosdec.balloon, has been modified from that listed in Tables 5 and 7 of [1]. Now both cylindrical and spherical balloons can be handled and each of these types of balloons can have either radial or truss-like (slanted) webs. Tables 5 and 7 of [1] are now out-of-date.

References:

- [1] Bushnell, David, “Use of GENOPT and BIGBOSOR4 to obtain optimum designs of a double-walled inflatable cylindrical vacuum chamber”, unpublished report, November, 2010
- [2] Sean A. Barton, “Stability Analysis of an Inflatable Vacuum Chamber”, *Journal of Applied Mechanics*, Vol. 75, No. 4, pp. xxxx-xxxx, July, 2008
- [3] Bushnell, David, "GENOPT--A program that writes user-friendly optimization code", *International Journal of Solids and Structures*, Vol. 26, No. 9/10, pp. 1173-1210, 1990. The same paper is contained in a bound volume of papers from the *International Journal of Solids and Structures* published in memory of Professor Charles D. Babcock, formerly with the California Institute of Technology.
- [4] Bushnell, David, "Stress, stability and vibration of complex, branched shells of revolution", *Computers & Structures*, vol. 4, pp 399-435 (1974)
- [5] Bushnell, D.: “BOSOR4 – Program for Stress Stability and Vibration of Complex, Branched shells of Revolution”, in *STRUCTURAL ANALYSIS SYSTEMS*, A. Niku-Lari, editor, Vol. 2, pp. 25-54, Pergamon Press, 1986
- [6] Bushnell, David, "Automated optimum design of shells of revolution with application to ring-stiffened cylindrical shells with wavy walls", AIAA paper 2000-1663, 41st AIAA Structures Meeting, Atlanta, GA, April 2000. Also see Lockheed Martin report, same title, LMMS P525674, November 1999
- [7] **a.** Bushnell, David and Thornburgh, Robert P., "Use of GENOPT and BIGBOSOR4 to optimize weld lands in axially compressed stiffened cylindrical shells and evaluation of the optimized designs by STAGS" AIAA Paper 2010-2927, 51st AIAA Structures, Materials and Dynamics Meeting, Orlando, FL, April, 2010. See also:
b. Bushnell, David, "Use of GENOPT and a BIGBOSOR4 "huge torus" model to optimize a typical weld land and weld land edge stringers in a previously optimized internally stiffened cylindrical shell without weld lands, unpublished report sent to NASA Langley Research Center, May 15, 2009.
- [8] **a.** Bushnell, D. and Rankin, C. “Use of GENOPT and BIGBOSOR4 to obtain optimum designs of an axially compressed cylindrical shell with a composite truss-core sandwich wall”, AIAA-2011-xxxx, 52nd AIAA

Structures meeting, Denver, CO, April, 2011. **b.** Bushnell, David, "Use of GENOPT and BIGBOSOR4 to obtain optimum designs of a cylindrical shell with a composite truss-core sandwich wall" Unpublished report for NASA Langley Research Center, June 20, 2009

[9] Bushnell, David, "Minimum weight design of imperfect isogrid-stiffened ellipsoidal shells under uniform external pressure", AIAA paper 2009-2702, 50th AIAA Structures Meeting, Palm Springs, CA, May 4-7, 2009

[10] Vanderplaats, G. N., "ADS--a FORTRAN program for automated design synthesis, Version 2.01", Engineering Design Optimization, Inc, Santa Barbara, CA, January, 1987

[11] Vanderplaats, G. N. and Sugimoto, H., "A general-purpose optimization program for engineering design", Computers and Structures, Vol. 24, pp 13-21, 1986

[12] Bushnell, David, "Recent enhancements to PANDA2" 37th AIAA Structures, Dynamics, and Materials (SDM) Conference, April 1996; AIAA Meeting Papers on Disc, 1996, pp. 126-182 A9626816, AIAA Paper 96-1337, In particular the section entitled, "INTRODUCTION OF A 'GLOBAL' OPTIMIZER IN PANDA2"

[13] Bushnell, David, the GENOPT file, /home/progs/genopt/doc/getting.started, which describes how to set up for executions of the GENOPT system.

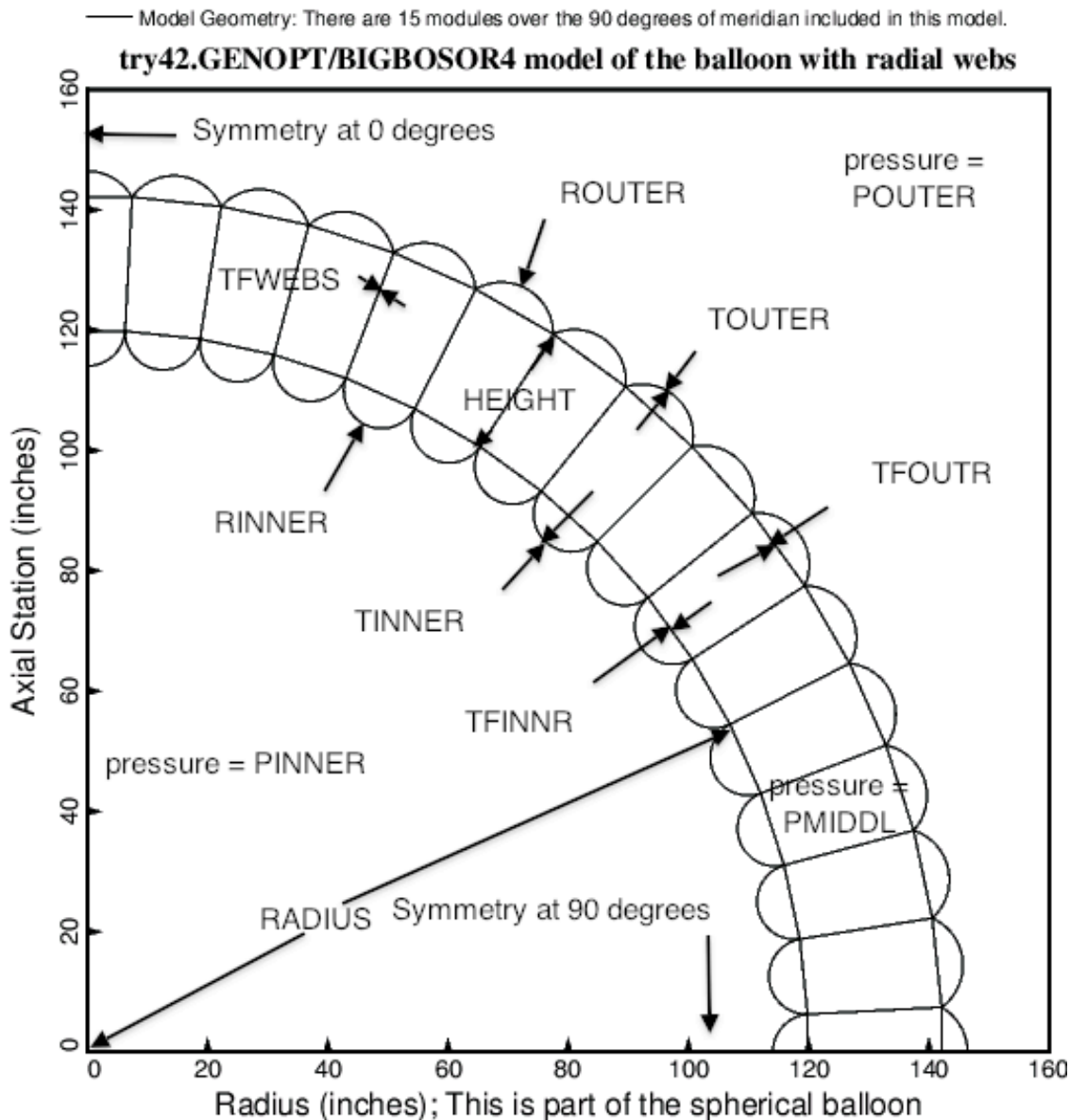


Fig. 1 Cross section of the “double” wall of the spherical vacuum chamber with **radial webs**. The radius to the inner wall is **RADIUS**, which is not a decision variable. The decision variable candidates are the distance between the inner and outer walls, **HEIGHT**, the two radii of curvature, **RINNER** and **ROUTER**, and the five thicknesses, **TINNER**, **TOUTER**, **TFINNR**, **TFOUTR**, and **TFWEBS**. The pressure inside the inner wall is **PINNER**; the pressure outside the outer wall is **POUTER**; the pressure between the inner and outer walls is **PMIDDL**. $PMIDDL > POUTER > PINNER$. The segments of the wall of thickness **TFINNR** and **TFOUTR** have little holes in them so that **PMIDDL** acts on both surfaces of them (no net pressure on them). Buckling of and stress in this configuration is computed with use of the **BIGBOSOR4** computer program. The wall is optimized (minimum weight) with the use of the system of computer programs called “**GENOPT/BIGBOSOR4**” [3, 6 – 9].

— Model Geometry: There are 15 modules over the 90 degrees of meridian included in this model.

try41.GENOPT/BIGBOSOR4 model of the balloon with truss-like webs

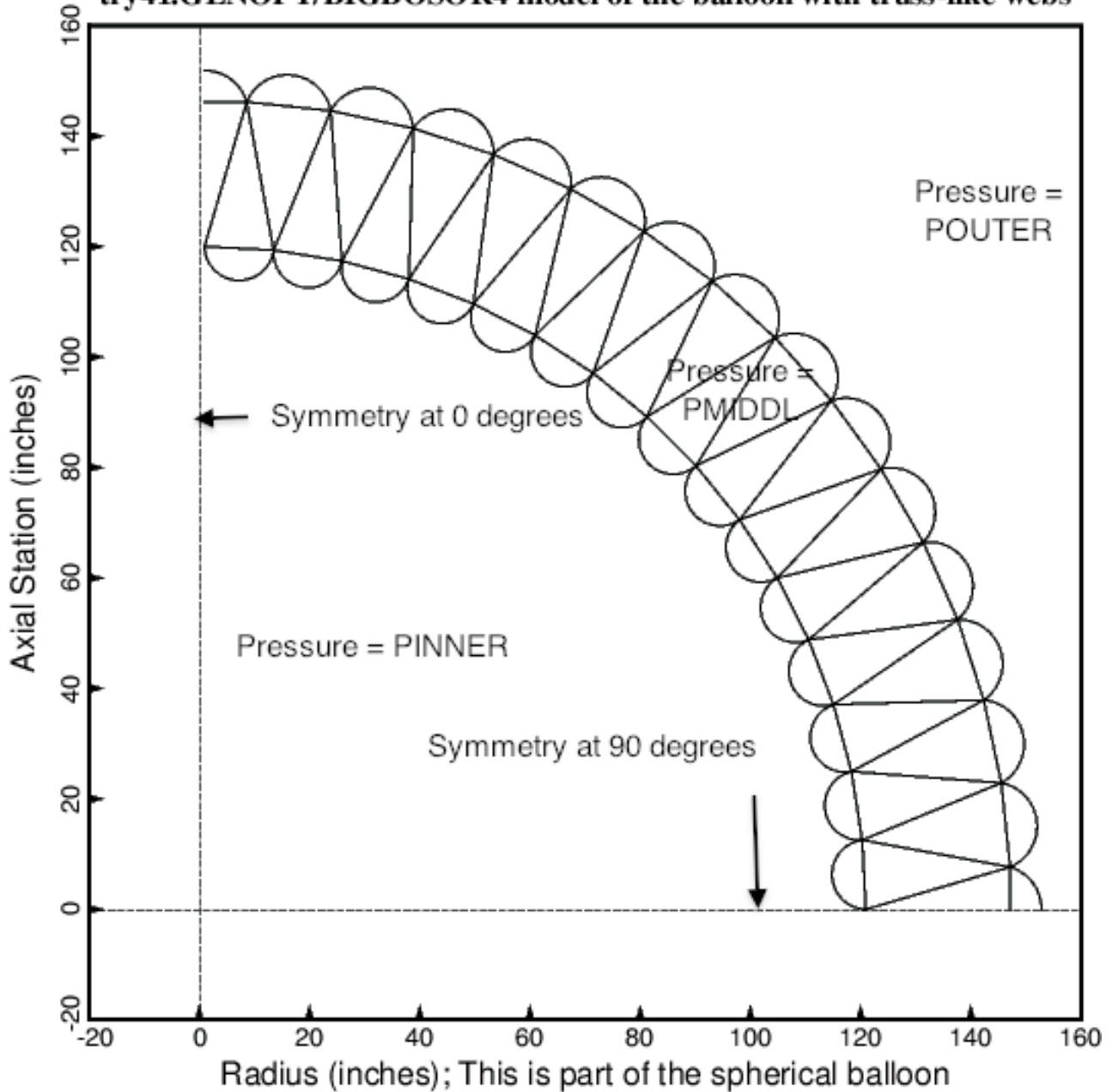


Fig. 2 Cross section of the double wall of the spherical vacuum chamber with **truss-like (slanted) webs**. The pressure inside the inner wall is PINNER; the pressure outside the outer wall is POUTER; the pressure between the inner and outer walls is PMIDDLE. $PMIDDLE > POUTER > PINNER$. The segments of the wall of thickness TFINNR and TFOUTR have little holes in them so that PMIDDLE acts on both surfaces of them (no net pressure on them). Buckling of and stress in this configuration is computed with use of the BIGBOSOR4 computer program. The wall is optimized (minimum weight) with the use of the system of computer programs called “GENOPT/BIGBOSOR4” [3, 6 – 9].

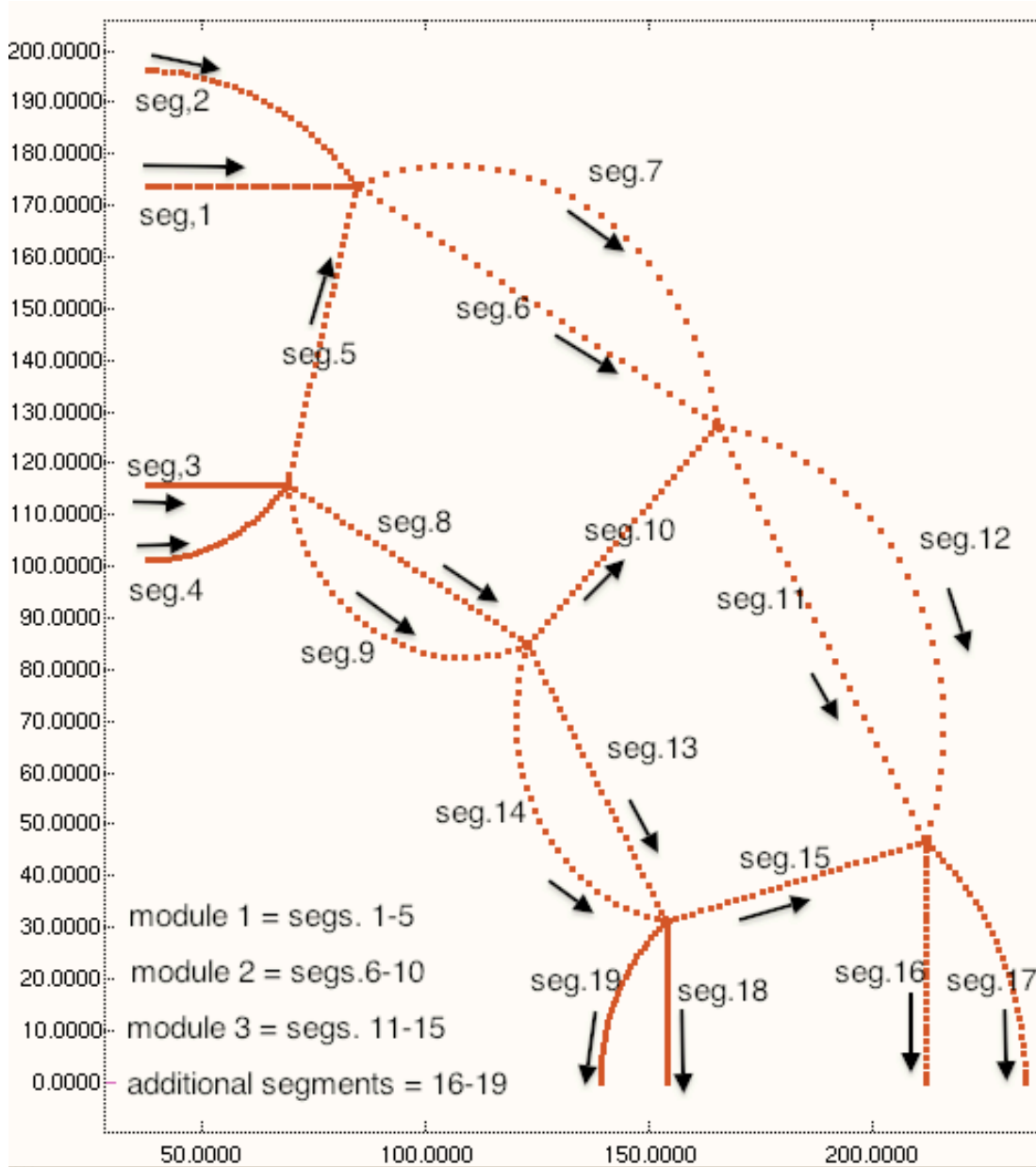


Fig. 3 (Taken from [1]). The complex wall of the cylindrical vacuum chamber (balloon) consists of a number of modules, NMODUL. NMODUL is an input quantity that the end user chooses when executing the GENOPT processor, BEGIN. In this crude model of a balloon wall **with radial webs** NMODUL = 3. The “shell” segment numbering convention and the direction of “travel” along each segment in the BIGBOSOR4 model are displayed here. Each “shell” segment is discretized in the meridional coordinate: 31 nodal points per segment. Variation of the buckling modal displacements in the direction normal to the plane of the paper is trigonometric. Although the computer program, BIGBOSOR4, was created to analyze shells with finite bending stiffness and the segments of the vacuum chamber treated in this paper act more like membranes than like shells, useful predictions are obtained. The same arrangements of modules and segments, the segment numbering scheme, and the direction of travel along each segment are used also for the spherical balloons.

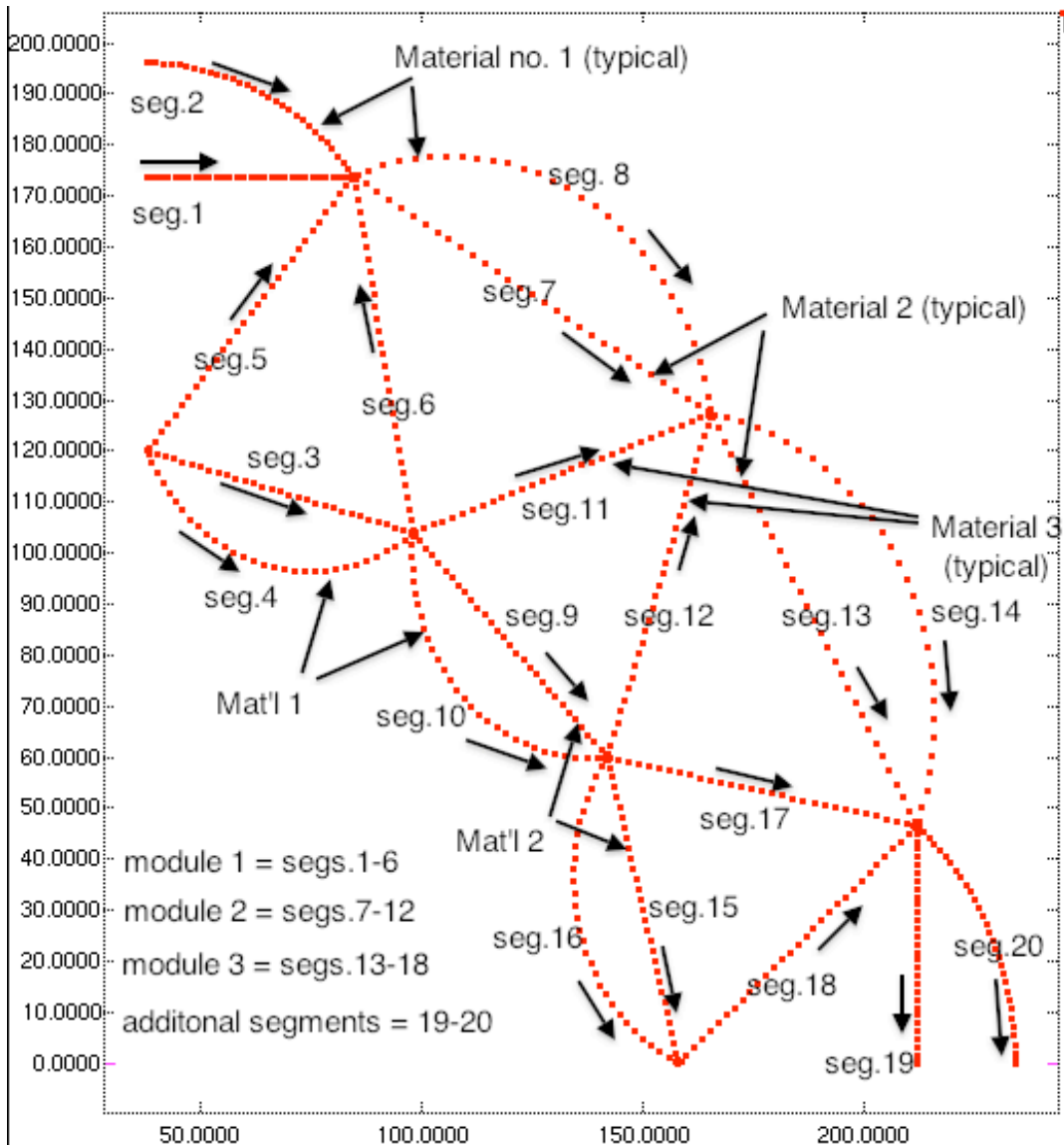


Fig. 4 (Taken from [1]). The complex wall of the cylindrical vacuum chamber (balloon) consists of a number of modules, NMODUL. NMODUL is an input quantity that the end user chooses when executing the GENOPT processor, BEGIN. In this crude model of a balloon wall **with truss-like (slanted) webs** NMODUL = 3. The “shell” segment numbering convention and the direction of “travel” along each segment in the BIGBOSOR4 model are displayed here. Each “shell” segment is discretized in the meridional coordinate: 31 nodal points per segment. Variation of the buckling modal displacements in the direction normal to the plane of the paper is trigonometric. There are 3 material types in this model and also in the model shown in the previous figure. In the studies reported in this paper all three material types have the same properties. Although the computer program, BIGBOSOR4, was created to analyze shells with finite bending stiffness and the segments of the vacuum chamber treated in this paper act more like membranes than like shells, useful predictions are obtained. The same arrangements of modules and segments, the segment numbering scheme, and the direction of travel along each segment are used also for the spherical balloons.

- Undeformed; There are 8 modules over 90 degrees of the meridian of the spherical balloon.
- Deformed: Axisymmetric (N=0 circumferential waves) buckling mode from BIGBOSOR4

try41. Bifurcation buckling from BIGBOSOR4; N=0; eigenvalue=3.4014

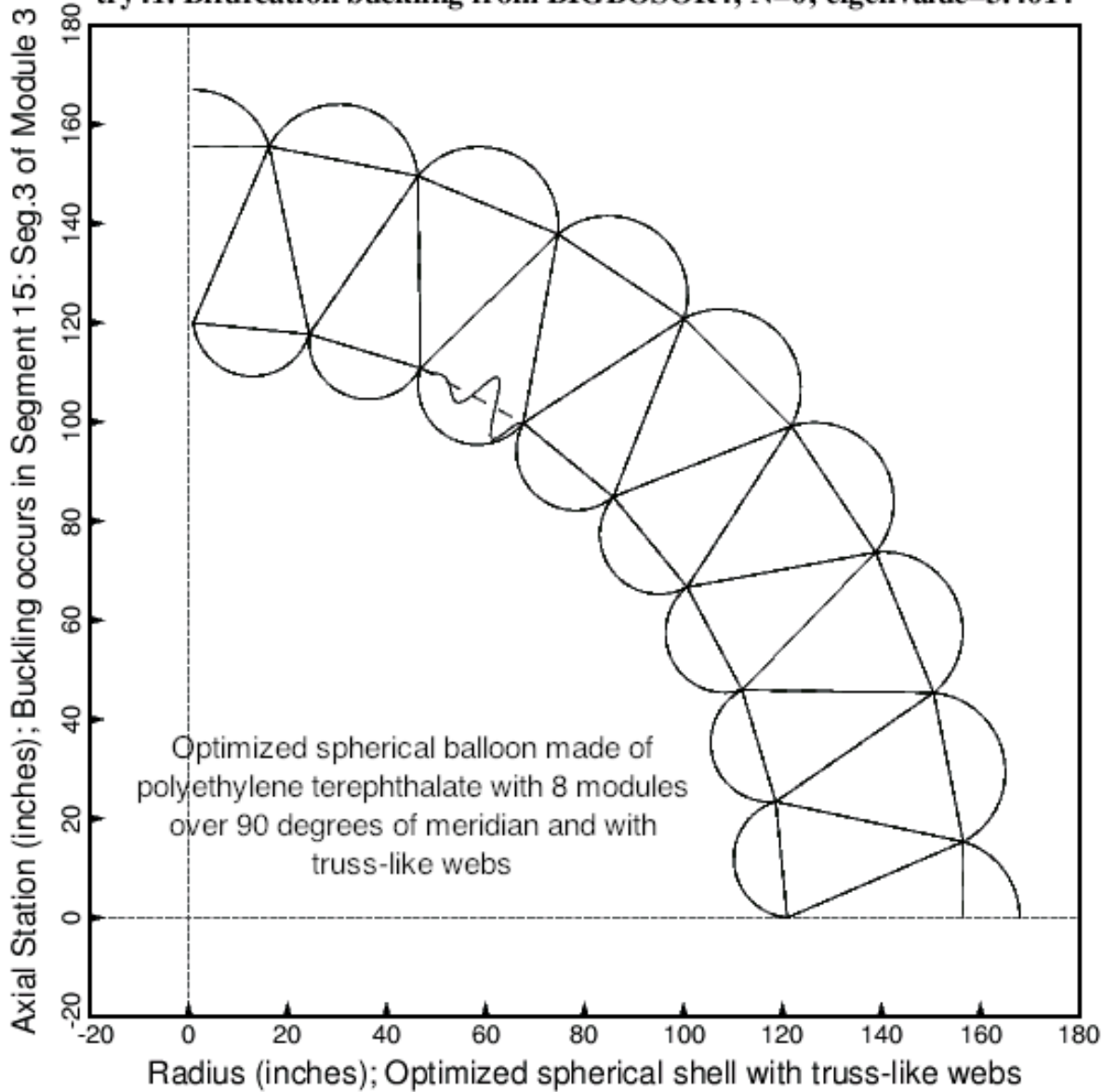


Fig. 10a Buckling mode shape of the optimized spherical balloon with 8 modules and truss-like (slanted) webs. This buckling mode, obtained from BIGBOSOR4, corresponds to $N = 0$ circumferential waves (axisymmetric buckling). Buckling first occurs in Segment 15, that is, in Segment 3 of Module 3. (Segment 15 = (2 modules) x 6 segments per module) + (3rd segment in Module 3). This location of the $N = 0$ buckling mode obtained from the BIGBOSOR4 stability analysis agrees with the prediction of the location of the initial loss of meridional tension as listed in **Item 10** of Table 9. During optimization cycles (ITYPE = 1 in the *.OPT file) only the $N = 0$ buckling mode from BIGBOSOR4 is computed in order to save computer time and because often there exist, especially for balloons made of strong material such as carbon fiber cloth, spurious non-axisymmetric buckling modes with very low eigenvalues. With ITYPE = 2 (analysis of a fixed design) a critical (minimum) buckling load factor is sought over a wide range of numbers of circumferential waves, N , as listed in **Item 9** of Table 9.

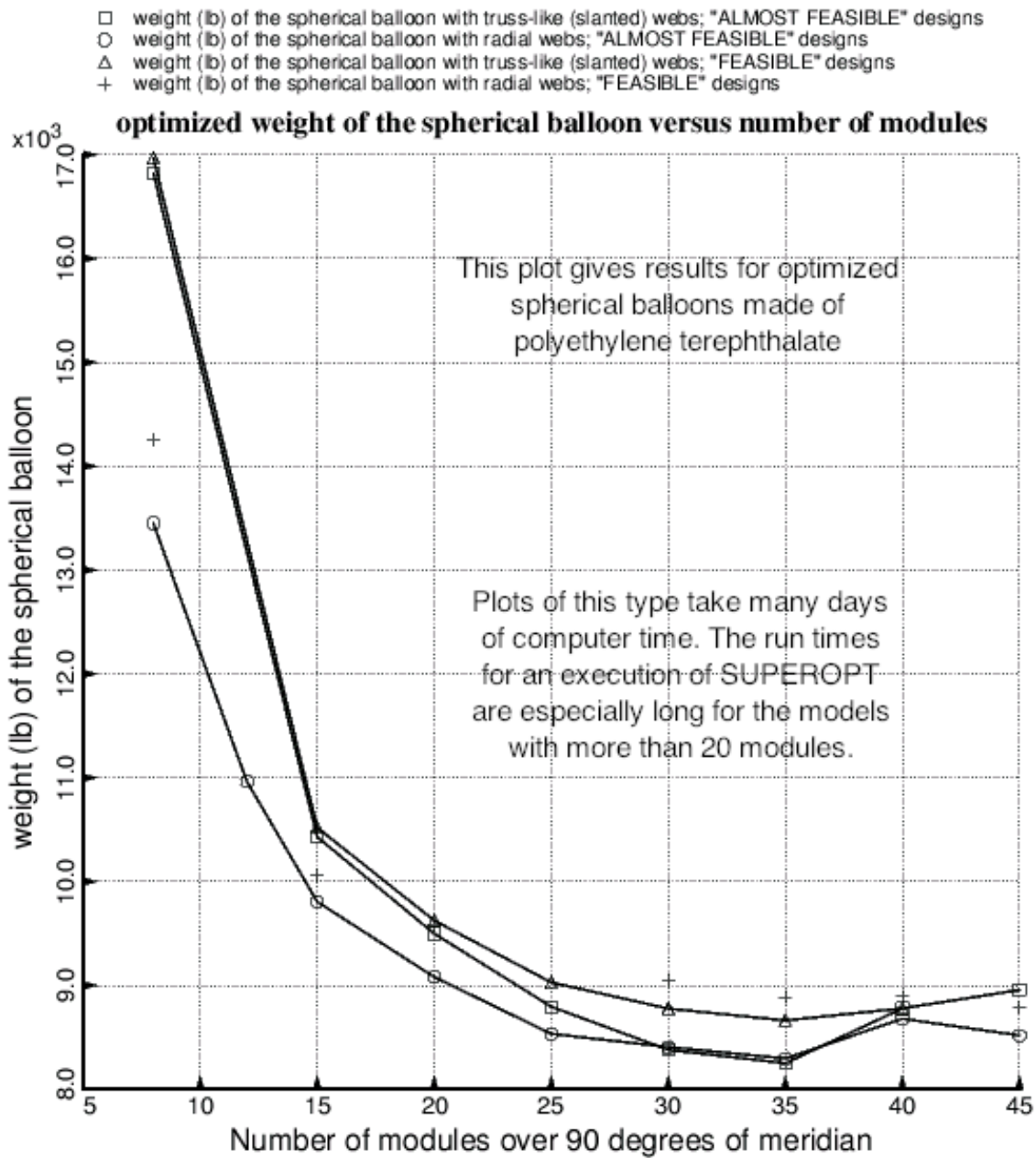


Fig. 23 The weight of optimized spherical balloons made of polyethylene terephthalate as a function of the number of modules over 90 degrees of meridian. All of the results in this figure were obtained with models in which there are 31 nodal points in each segment of the multi-module model. For the models with truss-like webs there are six segments per module plus two additional segments near the equator (Fig. 4). For models with radial webs there are five segments per module plus four additional segments near the equator (Fig.3). BIGBOSOR4 can handle up to 45 modules for models with truss-like webs and up to 55 modules for models with radial webs. For models with large numbers of modules the number of nodal points per segment is limited by the total number of degrees of freedom permitted by BIGBOSOR4 for pre-buckling analysis (20000 d.o.f) and for bifurcation buckling analysis (30000 d.o.f.). Compare this figure with Fig. 28.

- Undeformed; There are 35 modules over 90 degrees of the meridian of the spherical balloon.
- Deformed: axisymmetric (N=0 circumferential waves) buckling mode from BIGBOSOR4

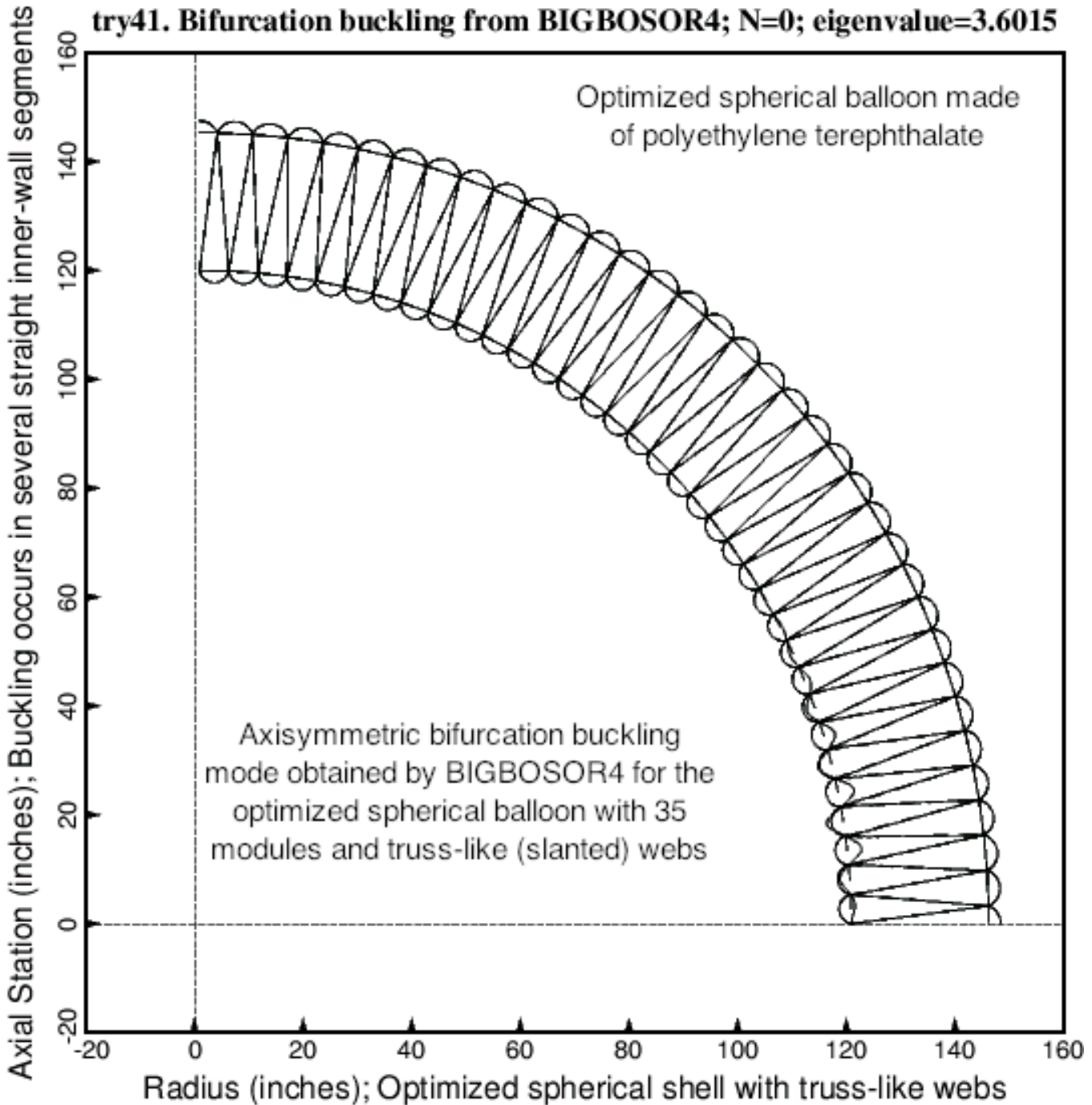


Fig. 24 Axisymmetric (N = 0 circumferential waves) buckling of the optimized spherical balloon with 35 modules over 90 degrees of meridian and with truss-like webs. As seen from the previous figure this configuration (35 modules, truss-like webs) corresponds to the spherical balloon with truss-like webs with the smallest optimized weight as a function of the number of modules.

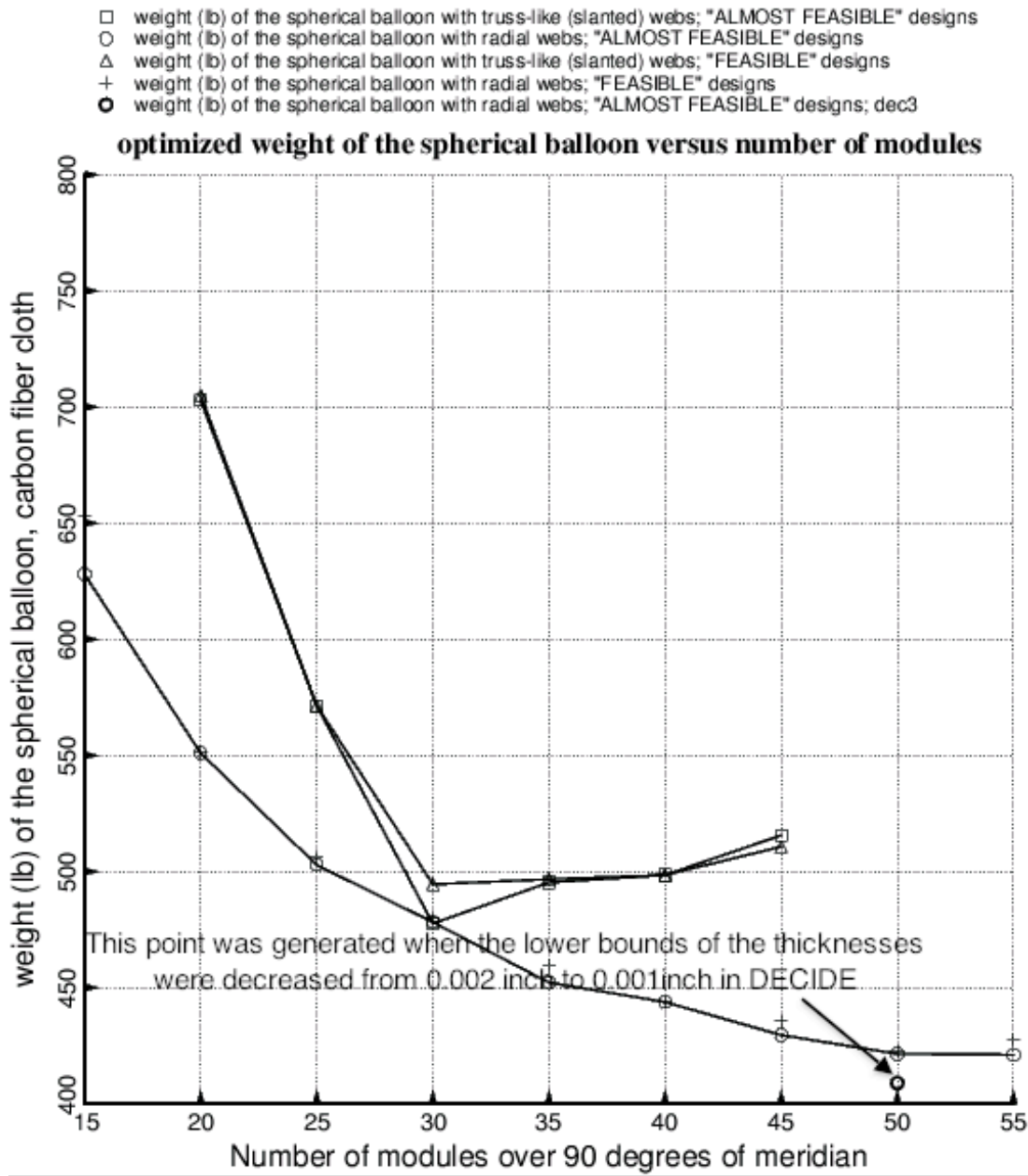


Fig. 28 The weight of optimized spherical balloons made of fictitious carbon fiber cloth as a function of the number of modules over 90 degrees of meridian. All of the results in this figure were obtained with models in which there are 31 nodal points in each segment of the multi-module model. For the models with truss-like webs there are six segments per module plus two additional segments near the equator (Fig. 4). For models with radial webs there are five segments per module plus four additional segments near the equator (Fig.3). BIGBOSOR4 can handle up to 45 modules for models with truss-like webs and up to 55 modules for models with radial webs. For models with large numbers of modules the number of nodal points per segment is limited by the total number of degrees of freedom permitted by BIGBOSOR4 for pre-buckling analysis (20000 d.o.f) and for bifurcation buckling analysis (30000 d.o.f.). Compare this figure with Fig. 23.

- weight/length (lb/in) of the cyl. balloon; truss-like (slanted) webs; "ALMOST FEASIBLE" designs
- weight/length (lb/in) of the cyl. balloon with radial webs; "ALMOST FEASIBLE" designs
- △ weight/length (lb/in) of the cyl. balloon; truss-like (slanted) webs; "FEASIBLE" designs
- + weight/length (lb/in) of the cyl. balloon with radial webs; "FEASIBLE" designs

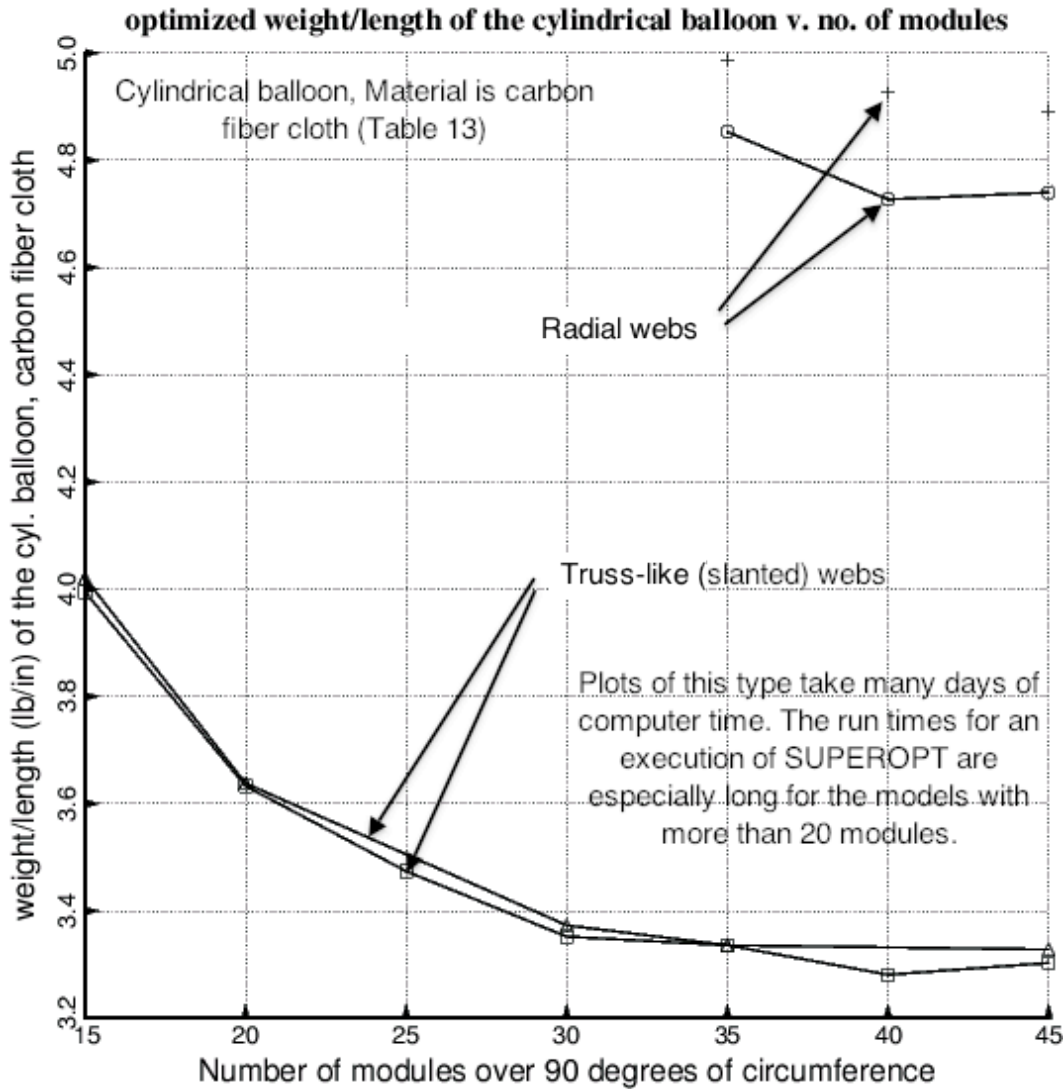


Fig. 56 The weight/length of optimized cylindrical balloons made of carbon fiber cloth as a function of the number of modules over 90 degrees of circumference. All of the results in this figure were obtained with models in which there are 31 nodal points in each segment of the multi-module model. For the models with truss-like webs there are six segments per module plus two additional segments near the circumferential coordinate, 90 degrees (Fig. 4). For models with radial webs there are five segments per module plus four additional segments near 90 degrees (Fig.3). BIGBOSOR4 can handle up to 45 modules for models with truss-like webs and up to 55 modules for models with radial webs. For models with large numbers of modules the number of nodal points per segment is limited by the total number of degrees of freedom permitted by BIGBOSOR4 for pre-buckling analysis (20000 d.o.f) and for bifurcation buckling analysis (30000 d.o.f.). Compare this figure with Fig. 25 of [1]. The optimized balloons made of carbon fiber cloth are about a factor of 17 lighter than those made of polyethylene terephthalate.

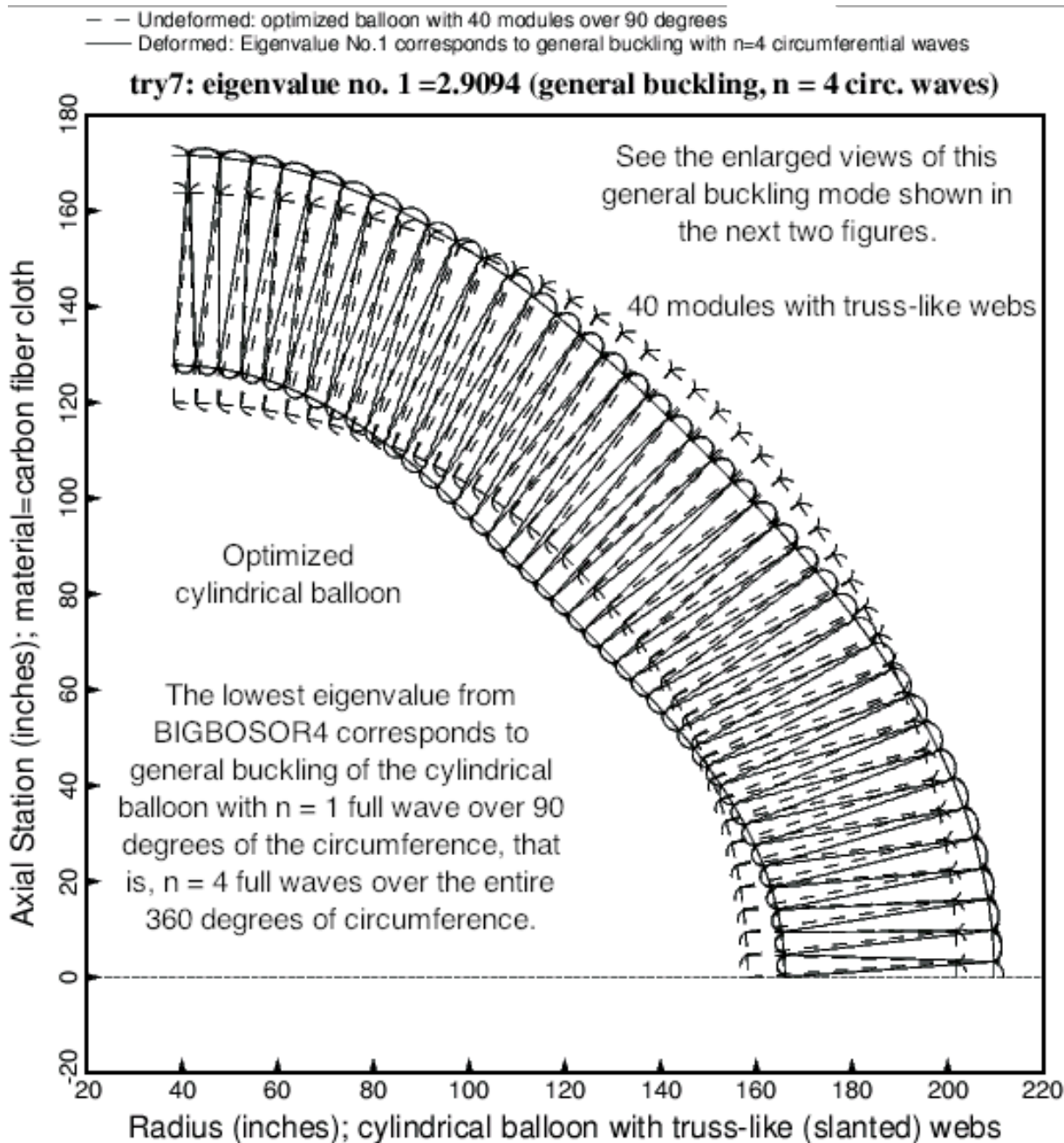


Fig. 65 General buckling of the optimized cylindrical balloon with 40 modules over 90 degrees of circumference and with truss-like webs. There are 31 nodal points in each segment of the model, which is the nodal point density specified in the “balloon” software, SUBROUTINE BOSDEC (NODSEG = 31) for optimization. This figure is analogous to Fig. 60. In this case BIGBOSOR4 produces an eigenvector that has a significant component of local spurious “zig-zag” buckling modal displacement. The question is: “Does the presence of the spurious ‘zig-zag’ component of buckling modal displacement significantly affect the critical buckling load factor (eigenvalue) predicted by BIGBOSOR4?” The answer from the predictions listed in Tables 21 and 22 appears to be, “no”.